Mon. Not. R. Astron. Soc. **390,** 839–846 (2008) doi:10.1111/j.1365-2966.2008.13794.x

Radio spectrum of the AXP J1810−197 and of its profile components

K. Lazaridis,[1⋆] A. Jessner,[1] M. Kramer,[2] B. W. Stappers,[2,3] A. G. Lyne,[2] C. A. Jordan,[2] M. Serylak[3,4] and J. A. Zensus[1]

[1]*Max-Planck-Institut für Radioastronomie, Auf dem Hügel 69, 53121 Bonn, Germany*
[2]*University of Manchester, Jodrell Bank Centre for Astrophysics, Alan-Turing Building, Manchester M13 9PL*
[3]*Stichting ASTRON, Postbus 2, 7990 AA, Dwingeloo, the Netherlands*
[4]*Astronomical Institute 'Anton Pannekoek', University of Amsterdam, Kruislaan 403, 1098 SJ Amsterdam, the Netherlands*

Accepted 2008 August 1. Received 2008 July 31; in original form 2008 June 20

ABSTRACT

As part of a European Pulsar Network (EPN) multitelescope observing campaign, we performed simultaneous multifrequency observations at 1.4, 4.9 and 8.4 GHz during 2006 July and quasi-simultaneous multifrequency observations from 2006 December until 2007 July at 2.7, 4.9, 8.4, 14.6 and 32 GHz, in order to obtain flux density measurements and spectral features of the 5.5 s radio-emitting magnetar AXP J1810−197. We monitored the spectral evolution of its pulse shape which consists of a main pulse (MP) and an interpulse (IP). We present the flux density spectrum of the average profile and of the separate pulse components of this first-known radio-emitting transient anomalous X-ray pulsar. We observe a decrease in the flux density by a factor of 10 within 8 m and follow the disappearance of one of the two main components. Although the spectrum is generally flat, we observe large fluctuations of the spectral index with time. For that reason, we have made some measurements of modulation indices for individual pulses in order to investigate the origin of these fluctuations.

Key words: stars: neutron – pulsars: general – pulsars: individual: AXP J1810−197.

1 INTRODUCTION

Magnetars, as first discussed by Duncan & Thompson (1992), are considered to be slowly rotating neutron stars with spin periods of 5–12 s and a rapid spin-down. They exhibit extremely strong magnetic fields, typically $>10^{14}$ G, the decay of which is believed to create the observable high X-ray and gamma-ray luminosities, often visible in bursts.

The model of magnetars tends to fit two previously described distinct classes of objects, the soft gamma-ray repeaters (SGRs) and the Anomalous X-ray pulsars (AXPs). Common properties of the members of both the classes are their long rotation periods (AXPs; Mereghetti & Stella 1995), (SGRs; Kouveliotou et al. 1999) and the bursting nature of their emission (Gavriil, Kaspi & Woods 2002; Kaspi et al. 2003). They are usually radio quiet. However, the pulsed radio emission that has been detected from AXP J1810−197 (Camilo et al. 2006) and AXP 1E1547.0−5408 (Camilo et al. 2008) indicates that this is not always the case.

The AXP XTE J1810−197 was discovered by Ibrahim et al. (2004) in *Rossi X-ray Timing Explorer* (*RXTE*) data of the source SGR 1806−20, taken in 2003 January. With a period of 5.54 s and a period derivative $\sim 1.15 \times 10^{-11}$ ss^{-1}, a magnetic field of $\sim 2.6 \times 10^{14}$ Gauss is implied. Although the previous observations clearly identified it as an AXP, the extreme variation in the X-ray flux also classified it as the first transient AXP.

The detection of a radio source coincident with the position of AXP J1810−197 by Halpern et al. (2005) first raised the possibility that this was the first radio-emitting magnetar. This possibility was confirmed with the detection of the strong, narrow and highly variable radio pulses, with the same pulse period as determined at high energies by Camilo et al. (2006). Further observations have shown that the emission is ∼80–95 per cent polarized, mostly linear, but with a significant degree of circular polarization at all observed frequencies (Camilo et al. 2007a; Kramer et al. 2007). One of the most remarkable features of the radio emission from this source is its flat radio spectrum. Radio pulsars are normally characterized by the steepness of their spectrum (Maron et al. 2000; Löhmer et al. 2008), which makes their detection at frequencies above 30 GHz very difficult. However, soon after the discovery of its radio emission, it became clear that AXP J1810−197 had a flat radio spectrum $S \propto \nu^{-0.5}$ (Camilo et al. 2006, 2007c) and for a time became the brightest neutron star at frequencies greater than about 40 GHz. Strong variations in the pulsed intensity and the profile phase were visible in the initial observations (Camilo et al. 2007b), although it also became evident that the average-pulsed flux density was decreasing with time.

In this paper, we report on the results of simultaneous and quasi-simultaneous multifrequency observations conducted at the radio frequencies of 1.41, 4.90 and 8.35 GHz during 2006 July and 2.64,

⋆E-mail: klazarid@mpifr-bonn.mpg.de

4.85, 8.35, 14.6 and 32 GHz from 2006 December to 2007 July. We present the radio spectrum of the total radio flux density of AXP J1810−197 and of its individual profile components and the results of power-law fits to this spectrum. We also consider the time variability of the fitted spectral index in light of the modulation of individual pulses and the intraday flux density variability. A full discussion of the individual pulse properties will follow in a separate paper.

2 OBSERVATIONS

The simultaneous observations were made using the 100-m radio telescope of the Max Planck Institute for Radioastronomy (MPIfR) at Effelsberg, Germany; the 76-m Lovell radio telescope at Jodrell Bank observatory of the University of Manchester, UK and the 94-m equivalent Westerbork Synthesis Radio Telescope (WSRT) in the Netherlands. The quasi-simultaneous observations were made with the Effelsberg radio telescope. In total, there were eight simultaneous multitelescope multifrequency sessions during 2006 July and 10 quasi-simultaneous multifrequency between 2006 December and 2007 July. For the latter sessions, the new subreflector of the Effelsberg telescope was used. It was installed in 2006 October, improving the sensitivity and resulting in flatter gain curves but also allowing fast receiver changes between secondary and primary focus. The integration time for every session depended on the observing frequency and on the observational circumstances. In general, the time needed for 1.42, 2.64, 4.85 and 4.90 GHz was around 5–15 min, for 8.35 GHz around 20 min and for 14.6 and 32 GHz around 25–40 min. The details of the observing sessions are summarized in Tables 1 and 2.

Table 1. Summary of simultaneous observing sessions in 2006 July.

Date	Session	Telescope	Frequency (GHz)	BW (MHz)
2006 May 31	1	Lovell	1.42	32
		WSRT	4.90	160
		Effelsberg	8.35	1000
2006 July 10	2	Lovell	1.42	32
		Effelsberg	8.35	1000
2006 July 17	3	Lovell	1.42	32
		WSRT	4.90	160
		Effelsberg	8.35	1000
2006 July 21	4	Lovell	1.42	32
		WSRT	4.90	160
2006 July 22	5	Lovell	1.42	32
		WSRT	4.90	160
		Effelsberg	8.35	1000
		Effelsberg	14.60	2000
2006 July 23	6	Lovell	1.42	32
		WSRT	4.90	160
2006 July 26	7	Lovell	1.42	32
		Effelsberg	4.85	500
		WSRT	4.90	160
		Effelsberg	8.35	1000
		Effelsberg	14.60	2000
2006 July 28	8	Lovell	1.42	32
		Effelsberg	4.85	500
		WSRT	4.90	160
		Effelsberg	8.35	1000
		Effelsberg	14.60	2000

Table 2. Summary of quasi-simultaneous observing sessions from 2006 December to 2007 July.

Date	Session	Telescope	Frequency (GHz)	BW (MHz)
2006 December 09	1	Effelsberg	2.64	100
			4.85	500
			8.35	1000
			14.60	2000
2006 December 26	2	Effelsberg	2.64	100
			4.85	500
			8.35	1000
			14.60	2000
2007 February 04	3	Effelsberg	2.64	100
			4.85	500
			8.35	1000
			14.60	2000
2007 February 06	4	Effelsberg	4.85	500
			32.00	2000
2007 February 12	5	Effelsberg	4.85	500
			14.60	2000
2007 February 17	6	Effelsberg	4.85	500
			8.35	1000
			14.60	2000
			32.00	2000
2007 February 18	7	Effeslberg	4.85	500
			8.35	1000
			14.60	2000
			32.00	2000
2007 March 26	8	Effelsberg	4.85	500
			14.60	2000
			32.00	2000
2007 May 05	9	Effelsberg	4.85	500
			8.35	1000
			32.00	2000
2007 July 06	10	Effelsberg	4.85	500
			8.35	1000
			14.60	2000

2.1 Calibration procedures

The observing and calibration procedures for Effelsberg data were the same for the simultaneous and quasi-simultaneous session. We used the 2.64, 4.85, 8.35, 14.6 and 32 GHz cooled High Electron Mobility Transistor (HEMT) receivers that are installed in the secondary focus (Karastergiou et al. 2001). In order to calibrate the flux density of a pulsar at the Effelsberg radio telescope reliably, a noise diode signal is injected into the wavefront following the horn synchronously with the pulse period in the beginning of each measurement (Fig. 2). The power output of the diode is compared with the power that is received from the pulsar. The signal of the noise diode itself is frequently calibrated and monitored by observing known reference sources during regular pointing observations. The sources that were used for calibration were 3C 273, 3C 274, 3C 286 and NGC 7027. They were observed at the beginning and end of each session, in combination with checks on the pointing and focus stability. The whole procedure of Effelsberg calibration is described further in Angelakis (2007). We also monitored the quality of our observations by taking data for well-known pulsars such as PSR B1929+10 which is strong enough to be detected at all frequencies up to 43 GHz. The observed properties of this pulsar, extensively also studied at Effelsberg, were compared to

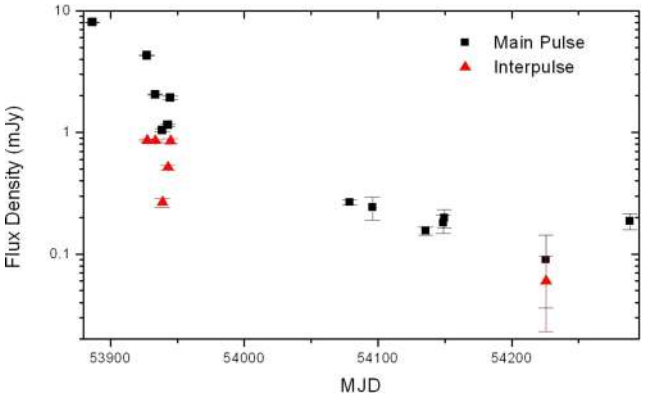

Figure 1. The average flux density for each observing session as measured at 8.35 GHz for the main pulse and the interpulse (when detected).

archival data to confirm that the system was functioning correctly at all frequencies. The observing and calibration procedures for the other telescopes participating in our simultaneous observations between 2006 May and July are described for each telescope in detail in Kramer et al. (2007).

3 DATA ANALYSIS AND RESULTS

Until 2006 August, the integrated pulse profile of AXP J1810−197 consisted of two major well-separated features which we discussed in some detail already in Kramer et al. (2007). Following the same convention, we refer to them as the *main pulse* (MP, right-hand side feature in Fig. 2a) and *interpulse* (IP, left-hand side feature in Fig. 2a). The MP is the more complex and wider of the two, with a varying width of about 0.7 s (or 45° in pulse longitude) while the IP is much narrower with a width of typically 0.2 s (or 12° longitude). In some cases, three or more distinct subcomponents were visible in the MP. The simpler IP was not always visible and was only strongly detected during parts of our observations, as indicated in Fig. 1 where we present the daily average flux densities of the two components as measured at 8.4 GHz as a function of time. The identification of the remaining visible pulse feature (see e.g. Fig. 2b) with the MP is possible due to timing information obtained from regular monitoring observations with the Lovell telescope at the Jodrell Bank observatory (Lyne et al., in preparation). After the disappearance of the IP in summer 2006, both MP and IP were visible again simultaneously only during one short session in 2007 May. The IP remains undetected since.

Overall, the flux density of the source has significantly decreased since its first detection at radio frequencies (see Fig. 1), which is consistent with the earlier findings by Camilo et al. (2007b). Due to the differences in the frequency range of the simultaneous and quasi-simultaneous observations, we discuss further results from these campaigns separately.

3.1 Simultaneous observations

The flux densities measured during the simultaneous observations and the spectral indices derived from power-law fits, $S \propto \nu^{\alpha}$ to these data, are listed in Tables 3 and 4 and shown in Figs 3 and 4. For each observation, we summed all individual pulses to obtain an integrated total power profile that was flux calibrated. The nominal conservative uncertainties for our flux density measurements are about 10 per cent (see also Section 3.2). In addition to our flux densities, we also utilize published flux densities measured at 1.42 and 4.8 GHz

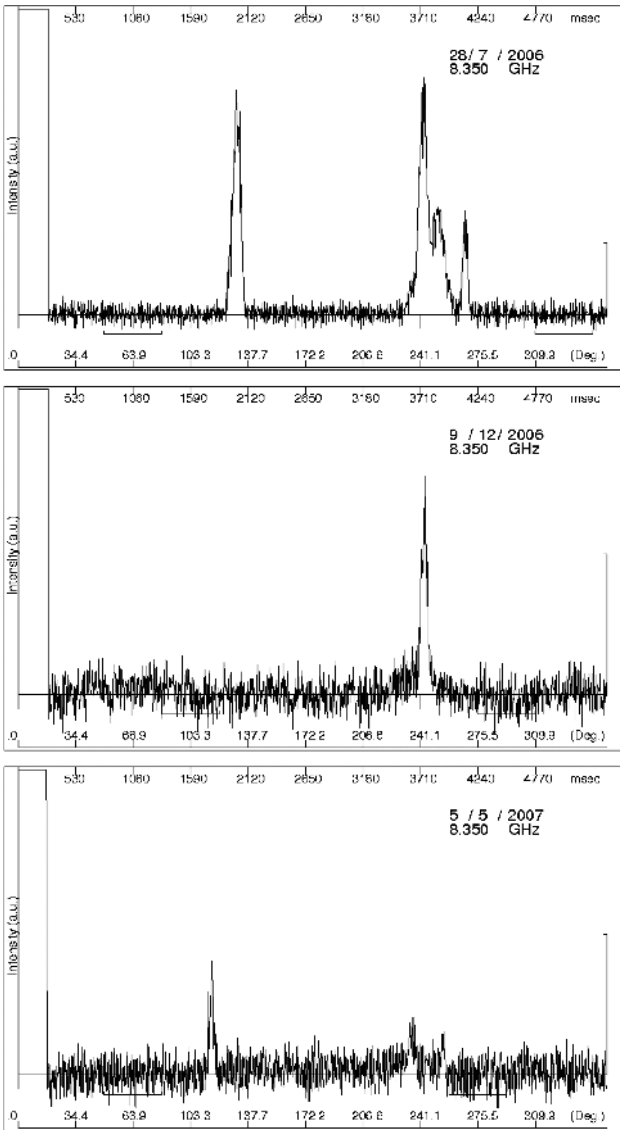

Figure 2. Phase aligned integrated profiles of AXP J1810−197 in 2006 July (top panel), 2006 December (middle panel) and 2007 May (bottom panel). The source becomes significantly weaker while the IP eventually disappears. Only in 2007 May, both the MP and IP are visible again. Note that each shown profile contains the signal of the calibrating noise diode which was switched on synchronously with the pulse period for the first 50 phase bins.

with the Very Large Array (VLA; Camilo et al. 2007c) and at 1.4 and 4.8 GHz at the Mount Pleasant observatory (Hotan et al. 2007) (see Fig. 3). Our flux densities observed for the MP at similar epochs for these frequencies are in good agreement with these values. This fact indicates that the effect of interstellar scintillation (ISS) may be small due to the large observing bandwidths, but we will discuss the possible impact of the interstellar medium on our results in more detail later. Overall, a large decrease in the signal strength with time is observed. At the same time, the spectrum is generally flat with an average spectral index of $\alpha = -0.31 \pm 0.06$ for the MP and $\alpha = -0.41 \pm 0.21$ for the IP (see Figs 3 and 4), consistent with results by Camilo et al. (2006, 2007c). However, around MJD 53938 (2007 July 22), we observe a strong time variability with the spectrum being initially steep and then flattening day by day for both MP and IP.

Table 3. Summary of flux densities and spectral indices for the main pulse.

Date	Frequency (GHz)	S_m (mJy)	α
2006 May 31	1.42	8.23 ± 0.82	$+0.01 \pm 0.11$
	4.90	9.73 ± 0.97	
	8.35	8.03 ± 0.01	
2006 July 10	1.42	6.90 ± 0.69	-0.27 ± 0.06
	8.35	4.28 ± 0.03	
2006 July 17	1.42	6.06 ± 0.61	-0.64 ± 0.14
	4.90	2.27 ± 0.23	
	8.35	2.05 ± 0.03	
2006 July 21	1.42	2.14 ± 0.21	-0.33 ± 0.11
	4.90	1.42 ± 0.14	
2006 July 22	1.42	2.59 ± 0.26	-0.79 ± 0.30
	8.35	1.04 ± 0.03	
	14.60	0.33 ± 0.03	
2006 July 23	1.42	3.24 ± 0.32	-0.55 ± 0.11
	4.90	1.61 ± 0.16	
2006 July 26	1.42	0.99 ± 0.10	-0.03 ± 0.11
	4.85	1.40 ± 0.03	
	4.90	0.86 ± 0.09	
	8.35	1.15 ± 0.03	
	14.60	1.06 ± 0.04	
2006 July 28	1.42	1.32 ± 0.13	0.15 ± 0.28
	4.85	1.66 ± 0.03	
	4.90	0.65 ± 0.06	
	8.35	1.92 ± 0.07	
	14.60	1.70 ± 0.04	

Table 4. Summary of flux densities and spectral indices for the interpulse.

Date	Frequency (GHz)	S_m (mJy)	α
2006 July 10	8.35	0.86 ± 0.02	–
2006 July 17	1.42	0.13 ± 0.01	$+1.12 \pm 0.33$
	4.90	0.83 ± 0.08	
	8.35	0.86 ± 0.02	
2006 July 21	4.90	0.44 ± 0.04	–
2006 July 22	4.90	0.58 ± 0.06	-1.61 ± 0.08
	8.35	0.27 ± 0.02	
	14.60	0.10 ± 0.04	
2006 July 23	4.90	0.58 ± 0.06	–
2006 July 26	4.85	0.81 ± 0.02	-1.29 ± 0.26
	8.35	0.51 ± 0.02	
	14.60	0.19 ± 0.03	
2006 July 28	1.42	0.49 ± 0.05	0.15 ± 0.28
	4.85	0.42 ± 0.02	
	4.90	0.28 ± 0.03	
	8.35	0.85 ± 0.04	
	14.60	0.58 ± 0.03	

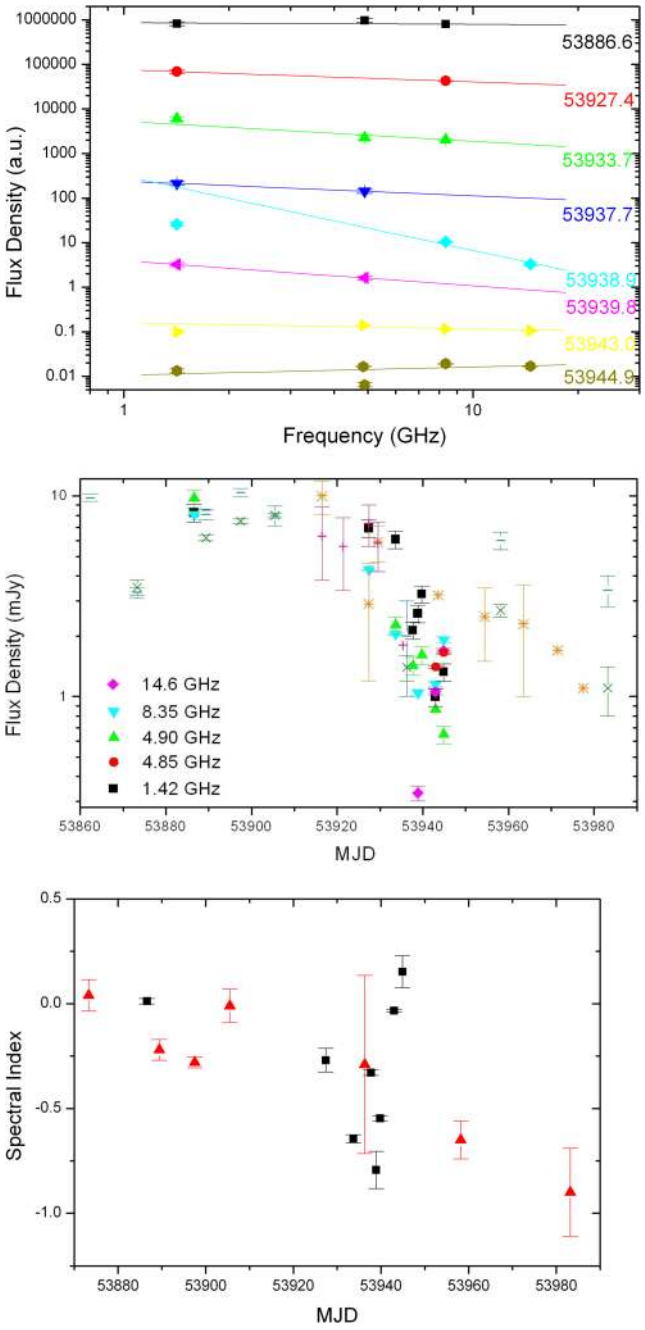

Figure 3. Top panel: flux density spectrum of the MP as determined during our simultaneous observations. For the plotting purposes, the flux densities of each day were multiplied by a different factor to distinguish the dates more clearly. Middle panel: flux density and its variability as measured at various frequencies as a function of time. We also added data measured by Hotan et al. (2007) at 1.4 and 4.8 GHz (shown as crosses and stars, respectively) and Camilo et al. (2007c) at 1.42 and 4.8 GHz (shown as bars and exes, respectively). Bottom panel: derived spectral indices of the MP as a function of time. The average value is determined $\alpha = -0.31 \pm 0.06$. In comparison, we show spectral indices derived by Camilo et al. (2007c) from VLA measurements as triangles.

3.2 Quasi-simultaneous observations

All quasi-simultaneous observations were performed with Effelsberg alone. The short time needed to switch between the different receivers (i.e. ∼30–60 s between secondary focus receivers, and ∼2–4 min between secondary and primary receivers) made it possible to observe at a wide range of frequencies in a single observing session. The longest multiwavelength observing session (without the calibration scans) of AXP J1810−197 was about 4 h, during which frequencies were cycled through repeatedly in order to detect any short-term variability. Using these data, we not only studied the long-term variability of AXP J1810−197, but also the medium

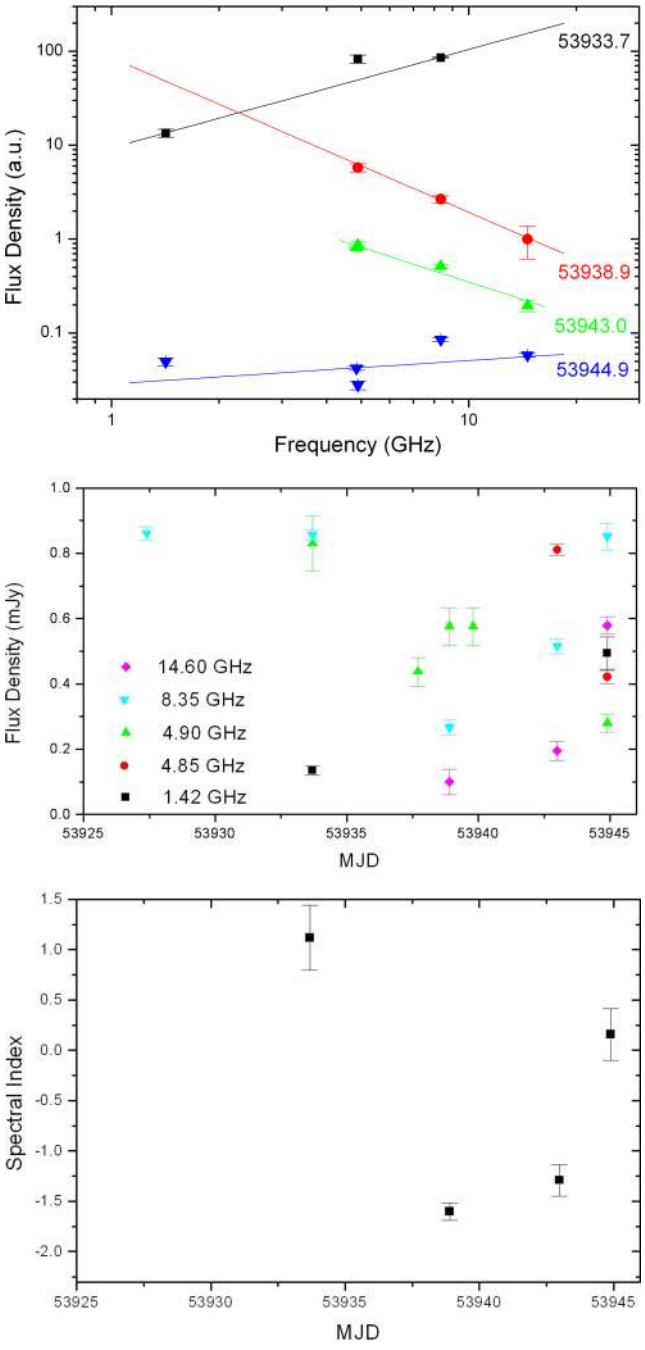

Figure 4. Top panel: flux density spectrum of the IP as determined during our simultaneous observations. For the plotting purposes, the flux densities of each day were multiplied by a different factor to distinguish the dates more clearly. Middle panel: flux density and its variability as measured at various frequencies as a function of time. Bottom panel: derived spectral indices of the IP as a function of time. The average value is determined $\alpha = -0.41 \pm 0.21$.

term intraday flux density fluctuations as well as the modulation of individual pulses during each of these sessions. An example of such measurements is shown in Fig. 5, where we present the flux density as measured repeatedly at 4.85 GHz over two consecutive days. The observed variation is consistent with a constant flux density over this period. The results of all our quasi-simultaneous observations are summarized in Table 5.

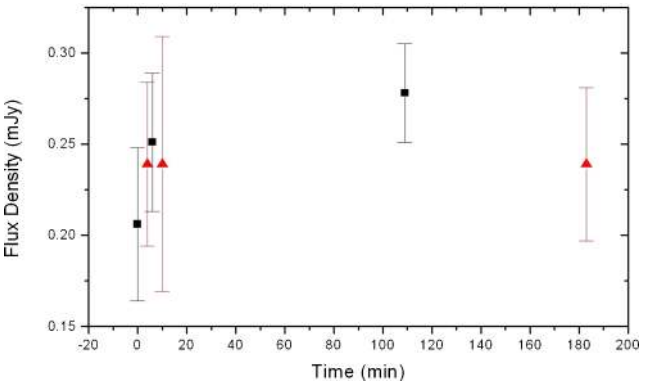

Figure 5. Flux density measured at 4.85 GHz during an observing session for two consecutive days (square and up triangle points). The first two measurements for each day correspond to a 5 min integration time while the third measurement corresponds to 15 min.

Table 5. Summary of flux densities and spectral indices for the MP measured during our quasi-simultaneous observing sessions.

Date	Frequency (GHz)	S_m (mJy)	α
2006 December 09	2.64	0.39 ± 0.05	-0.35 ± 0.11
	4.85	0.40 ± 0.03	
	8.35	0.27 ± 0.01	
	14.60	0.23 ± 0.03	
2006 December 26	2.64	0.56 ± 0.09	-0.67 ± 0.17
	4.85	0.25 ± 0.05	
	8.35	0.24 ± 0.05	
	14.60	0.16 ± 0.01	
2007 February 04	2.64	0.55 ± 0.08	-0.24 ± 0.49
	4.85	0.15 ± 0.05	
	8.35	0.15 ± 0.01	
	14.60	0.36 ± 0.03	
2007 February 06	4.85	0.20 ± 0.05	-0.18 ± 0.25
	32.00	0.14 ± 0.06	
2007 February 12	4.85	0.20 ± 0.03	0.11 ± 0.15
	14.60	0.22 ± 0.02	
2007 February 17	4.85	0.24 ± 0.02	$+0.06 \pm 0.13$
	8.35	0.18 ± 0.03	
	14.60	0.23 ± 0.01	
	32.00	0.25 ± 0.05	
2007 February 18	4.85	0.24 ± 0.03	$+0.03 \pm 0.08$
	8.35	0.20 ± 0.03	
	14.60	0.21 ± 0.02	
	32.00	0.25 ± 0.06	
2007 March 26	4.85	0.33 ± 0.03	-0.80 ± 0.17
	14.60	0.10 ± 0.02	
	32.00	0.08 ± 0.04	
2007 May 05	4.85	0.09 ± 0.03	$+0.86 \pm 0.27$
	14.60	0.09 ± 0.05	
	32.00	0.42 ± 0.08	
2007 July 06	4.85	0.15 ± 0.04	$+1.20 \pm 0.44$
	8.35	0.19 ± 0.03	
	14.60	0.55 ± 0.02	

The average flux density values were then used to determine the spectra and their indices. This was done for each session and the results are shown in Fig. 6. The results are consistent with and extend those of the simultaneous measurements. We find again

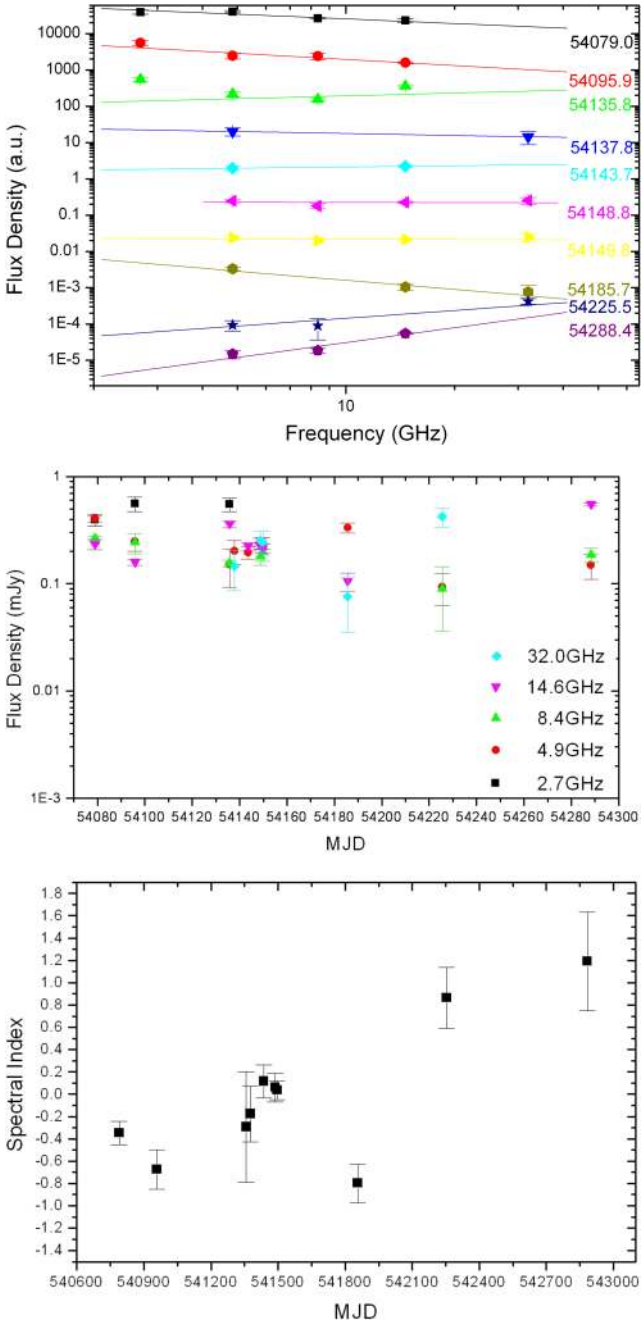

Figure 6. Top panel: flux density spectrum of the MP as determined during our quasi-simultaneous observations. For the plotting purposes, the flux densities for each day were multiplied by a different factor to distinguish the dates more clearly. Middle panel: flux density and its variability as measured at various frequencies as a function of time. Bottom panel: derived spectral indices of the MP as a function of time. The nominal average value is determined as $\alpha = -0.003 \pm 0.089$.

that the spectrum is generally flat with a mean spectral index of $\alpha = 0.00 \pm 0.09$ but it is also variable on a day-to-day basis with significant variations around its mean value. This is reflected also by the variation of the flux densities measured at 8.35 GHz and above which appear to sometimes follow a common pattern that is anticorrelated with changes seen below that frequency. There is an indication of a general increase in α over the 210 d covered by our observations, starting with initial values around $\alpha \sim -0.2$ and reaching $\alpha \sim 1.2$ near the end of the observing period.

3.3 Modulation indices

In order to characterize the observed flux density variations and to obtain reliable estimates for the measurement uncertainties, we also studied the modulation of the *single pulse* flux densities (see e.g. Kramer et al. 2003). We can use these results also to estimate the impact of the interstellar medium on our measurements, following similar studies such as that conducted for pulsars by Malofeev et al. (1996) at very similar frequencies, i.e. 4.75 and 10.55 GHz.

We concentrate on the flux densities measured at 4.85 and 14.6 GHz during our quasi-simultaneous sessions. The flux densities at these frequencies were measured in every session, often at the beginning and end of a session, providing a densely sampled data set that gives a good representation of the behaviour between widely spaced frequencies.

As a comparison, we also studied data for our reference source PSR B1929+10 to rule out systematic effects, impact of weather or instabilities in the receiver's chain. We find, as expected, only minor variations in the flux density of this well-known pulsar at high frequencies, in line with the findings of Malofeev et al. (1996).

For each session, we calculated the pulse-to-pulse modulation index m according to $m^2 = \frac{\langle (S-\langle S\rangle)^2\rangle}{\langle S\rangle^2} = \sigma_S^2/\langle S\rangle^2$ (e.g. Kramer et al. 2003), where S is the measured flux density, $\langle S\rangle$ its mean value and σ_S its standard deviation. We present the results in Fig. 7. As already expected from our discussion in Kramer et al. (2007) and consistent with early observations of AXP J1810−197 by Camilo et al. (2006), the pulses are very highly modulated and variable for both the frequencies. For the densely covered period of time around epoch MJD 54150 (2007 February 04–March 26), the data occasionally suggest a behaviour that is anticorrelated between 4.85 and 14.6 GHz. Overall, the higher frequency shows greater modulation, but it is possible that weaker single pulses are more difficult to detect at these frequencies. Despite this large modulation of the single pulses, averaging over sufficient time as done during all our observations essentially removes the variation for a given measurement value, leading to relative uncertainties in S of the order of $m/\sqrt{n}$, where n is the number of averaged pulses. This is consistent with our estimated flux density errors and confirmed by the

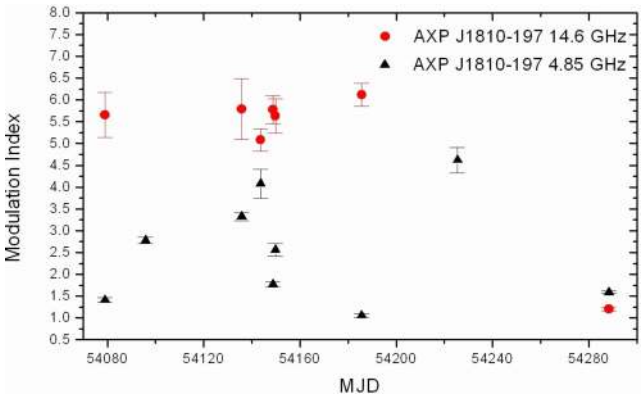

Figure 7. Variation of the pulse-to-pulse modulation index of AXP J1810−197 at 4.85 GHz (squares) and 14.6 GHz (triangle). At 14.6 GHz, the indices were computed for time-series covering 25–30 min while the 4.85 GHz data cover 10–30 min.

repeatability of our flux density measurements over consecutive days (see Fig. 5). We therefore expect the impact of slow-varying effects caused by refractive scintillation to be more important. We will discuss this in the following.

4 DISCUSSION

Our monitoring observations of AXP J1810−197 and its flux density spectrum over the course of more than 1 yr appear to confirm the conclusion derived already in all the previous studies of it that AXP J1810−197 behaves unlike most or even any known radio pulsar. Several observed properties support this fact. In our range of studied frequencies, the source exhibits a generally flat-flux density spectrum, with values of spectral index consistent with those measured by Camilo et al. (2006, 2007c). These flat spectra allowed us to observe the source up to very high frequencies, at least when compared to radio frequencies typically used for ordinary pulsar observations. An example is our detection of the magnetar at 43 GHz in 2007 May with the Effelsberg radio telescope. This is only the fifth neutron star detected at λ7 mm (Kramer et al. 1997) and the only one where single pulses could be observed. This is consistent with the observations at the IRAM 30 m telescope at 88 and 144 GHz by Camilo et al. (2007c), representing the highest radio frequency at which a neutron star has been detected. For normal pulsars, we often see breaks in their power-law spectra at high frequencies (Maron et al. 2000; Kijak, Gupta & Krzeszowski 2007) or even occasionally a turn-up at mm-wavelengths (Kramer et al. 1997). Here, in our range of frequencies, the spectrum of AXP J1810−197 is well described by a single, flat power law, of the form $S_\nu \propto \nu^\alpha$ with $\alpha = 0.0 \pm 0.5$.

In those cases where both the MP and IP were detected, their spectral indices were found to be differing, with the IP showing a significantly greater variation. Even though the spectra appear to change in the same manner from day to day, becoming steeper or flatter together, the IP exhibited many more extreme positive and negative steep values. This is somewhat surprising since the MP spectral index reflects emission from a wider range of emission components, in comparison to an IP that is always observed as a rather simple emission feature. The variation of the spectrum is roughly consistent with the model by Thompson (2008) where timescales of ∼0.1 d may be explained by current-driven instabilities on the closed magnetic field lines. The observation that it affects the IP and MP in a different way is interesting and may support the idea of a rather twisted magnetosphere. Although the spectrum is generally flat, the spectral index shows significant variation, with a slight trend of becoming more positive with time.

While we have shown that the effect of the significant pulse-to-pulse modulation can be removed by averaging a sufficient number of pulses, another well-known cause for flux density variations, and hence possible spectral index variations, is ISS. Based on the studies of the ISS at 4.75 and 10.55 GHz by Malofeev et al. (1996), the relatively large dispersion measure of DM = 178 pc cm^{-3}, and the estimated distance of 3.3 kpc, suggest a critical scintillation frequency f_c of ∼14 GHz, well within our observing band at 14.6 GHz. At this frequency, we may therefore expect a large variation of the measured flux density, whereas above the critical frequency we expect low flux density variations due to weak scintillation. Below f_c strong scintillation will occur, with a branch due to diffractive scintillation and one due to refractive scintillation. Lorimer & Kramer (2005) use a different functional dependence for the transition frequency which yields an $f_c \simeq 60$ GHz which agrees with the estimates by Camilo et al. (2007c) but is also smaller than $f_c \simeq 140$ GHz as derived from the NE2001 electron density model (Cordes & Lazio 2003). Despite these differences, the usage of large integration times and observing bandwidths will effectively average a number of scintils, resulting in reliable flux density measurements if bandwidth and integration time are sufficiently large. Following Lorimer & Kramer (2005) at 15 GHz, we estimate a diffractive scintillation bandwidth $\Delta\nu_d = 320$ MHz and a diffractive scintillation time-scale of $t_d = 600$ s which is in good agreement with the characteristics of features seen in the dynamic spectrum at the same frequency by Ransom et al. (2007). Our observations always average over several diffractive scintles in frequency and time, but will be affected by refractive scintillations at high frequencies. Around 15 GHz, the modulation index for refractive scintillations is estimated as $m_r = 0.6$ and the time-scale for refractive modulations turns out to be $t_r = 12.8$ h. Our observatories could not track the source for such a long time, so that we account for these possible variations with an increased quoted flux density error. For typical integration times of $t_{int} = 40$ min, our observing set-up should result in typical errors of our individual flux density measurements due to refractive and diffractive scintillations of about 20 per cent at 1.4 GHz, rising to a maximum of 77 per cent at 14.6 GHz and levelling off at about 62 per cent at 33 GHz and above. Similar estimates for the low-DM reference source PSR B1929+10 are in good agreement with the observations. We therefore conclude that the ISS plays a significant role in the individual flux density measurements, although it cannot be responsible for the pulse-to-pulse modulation index, and the described variations of the spectral index for different features of the profile between individual sessions.

Considering the overall flux density of AXP J1810−197, we can divide our observations, spanning more than a year, in four intervals. The first lasts until 2006 July when the average flux density from the source was above 6 mJy. The second lasted from 2006 July to September when the average flux density was above 1 mJy. The third epoch lasted from 2006 October to 2007 July when the flux density was below 0.5 mJy, and finally the time after 2007 July when the source became too weak for regular detection. At the same time, we observe a trend that the flux density variations are larger in the low-flux stages. This naturally makes the flux density spectrum computation less certain.

Due to the variability of the flux densities, it is difficult to compute an average spectrum. Especially when we inspect the flux density measurements from the third epoch, we see many cases in which the high and low frequencies vary in a completely different manner for the same day. As we have seen, some anticorrelation in flux density variations between high and low frequencies appears present, and given our discussion above, we consider these variations to be intrinsic to the source and not due to ISS. They can, in part, be explained by the assumption that we observe different components of the MP on different days. However, a similar variation is also observed for the IP, where always the same emission component is visible. Therefore, we conclude that in contrast to pulsars, the radio emission of magnetars is not intrinsically stable. That is consistent with the overall decay of the flux density in recent months and may indicate that the radio emission is a transient phenomenon that was triggered by the high-energy outburst. As the conditions for radio emission may revert to the pre-outburst stage, it will be interesting to monitor the source during and after the next outburst.

5 SUMMARY

As a result of a coordinated measurement campaign of three telescopes operating simultaneously at four different frequencies and

several daily Effelsberg measurements up to frequencies of 43 GHz, we find AXP J1810−197 to be an unusual pulsating radio source. Its spectral properties and temporal fluctuations differ remarkably from normal pulsars.

A complex picture of the variability of the radio flux density emerges as a result of our observations. The significant variability exists on all considered time-scales, from pulse to pulse, day to day and over the time of weeks and months, most of it being due to intrinsic variations (profile changes) and only some of it affected by scintillations.

Normal pulsars have stable average profiles enabling us to model their emission mechanism. This is, however, not possible with this source. Also the very flat spectrum and the visibility to high frequencies make the source unique among radio-emitting neutron stars.

ACKNOWLEDGMENTS

KL was supported for this research through a stipend from the International Max Planck Research School (IMPRS) for Astronomy and Astrophysics at the Universities of Bonn and Cologne. We especially thank Emmanouil Angelakis for the programming help and for the fruitful discussions. MS was supported by the EU Framework 6 Marie Curie Early Stage Training programme under contract number MEST-CT-2005-19669 'ESTRELA'.

REFERENCES

Angelakis E., 2007, PhD thesis, Univ. Bonn
Camilo F., Ransom S. M., Halpern J. P., Reynolds J., Helfand D. J., Zimmerman N., Sarkissian J., 2006, Nat, 442, 892
Camilo F., Reynolds J., Johnston S., Halpern J. P., Ransom S. M., van Straten W., 2007a, ApJ, 639, L37
Camilo F. et al., 2007b, ApJ, 663, 497
Camilo F. et al., 2007c, ApJ, 669, 561
Camilo F., Reynolds J., Johnston S., Halpern J. P., Ransom S. M., 2008, ApJ, 679, 681
Cordes J. M., Lazio T. J. W., 2003, preprint (astro-ph/0207156)
Duncan R. C., Thompson C., 1992, ApJ, 392, L9
Gavriil F. P., Kaspi V. M., Woods P. M., 2002, Nat, 419, 142
Halpern J. P., Gotthelf E. V., Becker R. H., Helfand D. J., White R. L., 2005, ApJ, 632, L29
Hotan A. W., Long S. R., Dickey J. M., Dolley T. J., 2007, ApJ, 668, 449
Ibrahim A. I. et al., 2004, ApJ, 609, L21
Karastergiou A. et al., 2001, A&A, 379, 270
Kaspi V. M., Gavriil F. P., Woods P. M., Jensen J. B., Roberts M. S. E., Chakrabarty D., 2003, ApJ, 588, L93
Kijak J., Gupta Y., Krzeszowski K., 2007, A&A, 462, 699
Kouveliotou C. et al., 1999, ApJ, 510, L115
Kramer M., Jessner A., Dorosenko O., Wielebinski R., 1997, ApJ, 488, 364
Kramer M., Karastergiou A., Gupta Y., Johnston S., Bhat N. D. R., Lyne A. G., 2003, A&A, 407, 655
Kramer M., Stappers B. W., Jessner A., Lyne A. G., Jordan C. A., 2007, MNRAS, 377, 107
Löhmer O., Jessner A., Kramer M., Wielebinski R., Maron O., 2008, A&A, 480, 623
Lorimer D. R., Kramer M., 2005, Handbook of Pulsar Astronomy. Cambridge Univ. Press, Cambridge
Malofeev V. M., Shishov V. I., Sieber W., Jessner A., Kramer M., Wielebinski R., 1996, A&A, 308, 180
Maron O., Kijak J., Kramer M., Wielebinski R., 2000, A&AS, 147, 195
Mereghetti S., Stella L., 1995, ApJ, 442, L17
Ransom S. et al., 2007, Pulsar Searching and Thai-ming, 2007-SKA. Nat. Astr. Res. Inst. of Thail., Thailand
Thompson C., 2008, ApJ, submitted (arXiv:0802.2571)

This paper has been typeset from a TEX/LATEX file prepared by the author.